Time-lapse estimation for optical telescope sequences

Mark Campbell, Daniel E Clark

Time-Lapse Estimation for Optical Telescope Sequences
Estimation par Intervalle de Temps pour les Séquences de Télescopes Optiques

***Mark Campbell*[1] *and Daniel Clark*[2]**

[1] *School of Engineering and Physical Sciences, Heriot-Watt University, Edinburgh, United Kingdom, mc318@hw.ac.uk*
[2] *Télécom SudParis, Institut Mines-Télécom, daniel.clark@telecom-sudparis.eu*

Keywords: Sensor Calibration, Multi-Target Tracking
Mots-clefs: Calibrage du Capteur, Suivi Multi-Cible

Abstract:
Typical tracking scenarios rely on the assumption that there is a constant time lapse between observations. In real life applications, this assumption is often untrue. In Space Situational Awareness (SSA) applications accurate target estimation is of importance to obtain orbital information. This paper presents recent developments in multi target detection and tracking techniques, exploiting the Single Cluster Probability Hypothesis Density (SC-PHD) filter, in order to jointly estimate the dynamic objects and the time lapse between images.

Résumé:
Les scénarios de suivi typiques reposent sur l'hypothèse qu'il y a un laps de temps constant entre les observations. Dans les applications réelles, cette hypothèse est souvent fausse. Dans les applications SSA, l'estimation précise de la cible est importante pour obtenir des informations orbitales. Cet article présente les développements récents dans les techniques de détection et de suivi de cibles multiples, en exploitant le filtre SC-PHD, afin d'estimer conjointement les objets dynamiques et le laps de temps entre les images.

1 Introduction

The usage of low cost ground-based Complementary Metal Oxide Semiconductor (CMOS) optical sensors to track objects in Low Earth Orbit (LEO) and Geostationary Earth Orbit (GEO) has dramatically increased in popularity in the past decade, leading to a chance of integrating these sensors into the formal SSA environment. These Consumer Off-The-Shelf (COTS) cameras and optics are inexpensive solutions and provide a relatively wide Field of View (FoV). A central challenge in the exploitation of these sensors is the extraction of multiple detections from a single image due to the wide FoV: some detections can stem from moving objects (e.g. satellites, debris), some others from statics objects (e.g. stars), some of them may be artefacts from the extraction process or *false alarms*. The association between the objects and the detections is unknown, as are the number of objects, both static and moving, in the FoV. In these conditions, exploiting the output of a sensor in order to estimate the number and trajectories of the detected objects becomes a multi-object estimation problem.
The Probability Hypothesis Density (PHD) filter [1] was designed as an inexpensive filtering solution in the the context of multi-object filtering. Extensions to the PHD filter such as the Second-Order Probability Hypothesis Density (SO-PHD) [2] and the Cardinalized Probability Hypothesis Density (CPHD) [3] provide additional information at the expense of computational complexity. Solving this multi-object scenario is crucial so that methods such as Initial Orbit Determination (IOD) and astrometry can take place.
The multi-target tracking methods assume a constant time-lapse between observations e.g. a constant time between image captures. However this is often not the case when operating on real datasets. This could be due to a number of reasons: operator error, corrupted or missing metadata or even sensor failure. This paper explores the exploitation of multi-object tracking algorithms developed from the Finite Set Statistics (FISST) framework [1], known as the SC-PHD filter [4, 5], in order to jointly estimate the time-lapse between the images and the objects' states in a sequence of images produced from an optical sensor. Variations of this method have been used to register microscopy [6] and astronomy [7] images.
This paper is organized as follows. Sec. 2 presents the principle of joint multi-object filtering and sensor state estimation, and introduces the two multi-object filters exploited in the paper. Sec. 3 presents the details employed for the implementation of the algorithms. Sec. 4 describes the simulation tests and Sec. 5 discusses the results. Finally, the conclusions are provided in Sec. 6.

2 Joint Multi-Object Filtering and Sensor State Estimation

2.1 Single Cluster Probability Hypothesis Density (SC-PHD) filter

The joint calibration and tracking method exploits a Simultaneous Localisation and Mapping (SLAM) based approach [4] known as the Single Cluster Probability Hypothesis Density (SC-PHD) filter. There are two sources

of uncertainty to be estimated, represented by two different *processes*:

- The sensor process Ψ estimates the sensor state: in this application, the time-lapse between subsequent images,
- The object process Φ estimates the number and states of moving objects: in this application, the orbiting objects moving through the image sequence.

Since the number and states of the objects is assumed unknown and possibly varying across the image sequence, the object process Φ is estimated through multi-object filters derived from the FISST framework: in the scope of this paper, the PHD filter [1] and the SO-PHD filter [2] [8]. These two solutions are explained in more details in Sec. 2.2.

2.2 Multi Object Filtering

This section focuses on the estimation of the object process Φ As seen in Sec. 2.1, the estimation of the object process is conditioned upon the sensor state (i.e. time lapse between observations). In practical terms, a multi-object filter estimating the object process is maintained for each possible sensor state y. In this section, y_k denotes an arbitrary sensor state[1] at time k (i.e., in the k-th image of the sequence). Each object is described by its state x in the *(single) target state space* $\mathcal{X} \subseteq \mathbb{R}^d$, describing the physical characteristics of the object. An object may enter or leave the sensor FoV at any time during the image sequence, and thus the number of objects at any time is unknown and needs to be estimated. The multi-object state is represented by a Random Finite Set (RFS) Φ_k, a random object whose size and elements are unknown, and whose realization is a set of target states $X_k = \{x_1, x_2, ..., x_{n_k}\}$ represents a specific *multi-object configuration* at time k [3]. The evolution of the objects' state between time step $k-1$ and k is described by a Markov transition function $t_{k|k-1}$. The number and states of newborn objects is described by a RFS $\Phi_{\mathrm{b},k}$ whose nature depends on the filter; its *first-order moment density* or *intensity* is denoted by $\mu_{\mathrm{b},k}(\cdot)$.
An observation collected from the sensor is described by a state z in the *observation space* $\mathcal{Z} \subseteq \mathbb{R}^d$. The set of collected observation is denoted by Z_k, which contains observations of all the targets in the image at time k. The observation process is plagued by observation noise, missed detections, and false alarms. The observation noise associated to some collected observation z is characterized by the *likelihood* function $\ell_{z,k}(\cdot|y)$, while the probability of detection for each individual object in the sensor FoV is denoted by $p_{\mathrm{d},k}(\cdot|y)$. The number and states of false alarms is described by a RFS $\Phi_{\text{ɜ},k}$ whose nature depends on the filter; its intensity is denoted by $\mu_{\text{ɜ}k}(\cdot|y)$, and its spatial distribution is denoted by $s_{\text{ɜ},k}(\cdot|y)$. For the rest of the paper, the notation $\mu(\mathcal{X})$ will be used for various intensity functions μ to denote the integral $\int_{\mathcal{X}} \mu(x)\mathrm{d}x$.

2.2.1 Probability Hypothesis Density (PHD) Filter

The PHD filter [1] was designed as an inexpensive filtering solution in the the context of multi-object filtering, propagating only the intensity μ_k of the object process Φ_k. The key assumptions of the PHD filter is that both the predicted process $\Phi_{k|k-1}$ and false alarm process $\Phi_{\text{ɜ},k}$ are Poisson [1]. The prediction and update steps of the PHD filter are given by

$$\mu_{k|k-1}(x|y) = \mu_{\mathrm{b},k}(x) + \mu_{\mathrm{s},k|k-1}(x|y), \tag{1}$$

$$\mu_k(x|y) = \mu_{\phi,k}(x|y) + \sum_{z \in Z_k} \frac{\mu_{z,k}(x|y)}{\mu_{\text{ɜ}k}(z|y) + \mu_{z,k}(\mathcal{X}|y)}, \tag{2}$$

where the *survival* $\mu_{\mathrm{s},k|k-1}(x|y)$, *missed detection* $\mu_{\phi,k}(x|y)$, and *association* $\mu_{z,k}(x|y)$ terms are defined as

$$\mu_{\mathrm{s},k|k-1}(x|y) = \int p_{\mathrm{s},k}(\bar{x}) t_{k|k-1}(x|\bar{x}) \mu_{k-1}(\bar{x}|y)\mathrm{d}\bar{x}, \tag{3}$$

$$\mu_{\phi,k}(x|y) = (1 - p_{\mathrm{d},k}(x|y))\, \mu_{k|k-1}(x|y), \tag{4}$$

$$\mu_{z,k}(x|y) = p_{\mathrm{d},k}(x|y) \ell_{z,k}(x|y) \mu_{k|k-1}(x|y). \tag{5}$$

2.3 Second-Order Probability Hypothesis Density (SO-PHD) Filter

Recently, a second-order version of the PHD filter was introduced in [2] that combats some of the issues posed by the restrictive Poisson assumptions of the PHD filter. It propagating not only the intensity μ_k of the object process Φ_k, but also the variance $\mathrm{var}_k(\mathcal{X})$ of the number of objects in the whole target state space $\mathcal{X}$.
The SO-PHD filter substitutes Panjer assumptions to Poisson assumptions in the PHD filter, thus providing more flexibility in the description of the number of objects and false alarms. More specifically, the Panjer

[1] The estimator associated to the sensor state will be presented later in Sec. 2.4

distribution [2] describes the Poisson, binomial and negative binomial distributions in a unified formulation involving two parameters α and β which stand in one-to-one correspondence with the mean and variance of the distribution. Using this property, the SO-PHD filter is able to propagate the variances in the number of objects and number of false alarms via the Panjer parameters of the corresponding distributions.
Before stating the recursion of the SO-PHD filter, some notations inspired by those introduced in [9] for the CPHD filter will be states. The *Pochhammer symbol* or *rising factorial* $(\zeta)_n$ for any $\zeta \in \mathbb{R}$ and $n \in \mathbb{N}$ is defined with

$$(\zeta)_n := \zeta(\zeta+1)\cdots(\zeta+n-1), \quad (\zeta)_0 := 1. \tag{6}$$

Let $\alpha_{k|k-1}, \beta_{k|k-1}$ and $\alpha_{\text{ȝ},k}, \beta_{\text{ȝ},k}$ be the parameters of the predicted object process and clutter process at time k, respectively, and define the expression

$$Y_u^\flat[Z] := \sum_{j=0}^{|Z|} \frac{(\alpha_{k|k-1})_{j+u}}{(\beta_{k|k-1})^{j+u}} \frac{(\alpha_{\text{ȝ},k})_{|Z|-j}}{(\beta_{\text{ȝ},k}+1)^{|Z|-j}} F_{\text{d}}^{-j-u} e_j^\flat(Z) \tag{7}$$

for any $Z \subseteq Z_k$ and for $u = 1, 2$, where F_{d} is the scalar

$$F_{\text{d}} := \int \left[1 + \frac{p_{\text{d},k}(x|y)}{\beta_{k|k-1}}\right] \mu_{k|k-1}(x|y)\text{d}x, \tag{8}$$

and the so-called *elementary symmetric functions* [10] $e_j^\flat$ are given by

$$e_j^\flat(Z) := \sum_{\substack{Z' \subseteq Z \\ |Z'|=j}} \prod_{z \in Z'} \frac{\mu_{z,k}(\mathcal{X}|y)}{s_{\text{ȝ},k}(z|y)}. \tag{9}$$

Where $s_{c,k}$ denotes the spatial clutter distribution at time k. With the help of Eq. (7), define the *corrective terms* via

$$l_u^\flat(\phi|y) := \frac{Y_u^\flat[Z_k]}{Y_0[Z_k]} \quad \text{and} \quad l_u^\flat(z|y) := \frac{Y_u^\flat[Z_k \backslash \{z\}]}{Y_0^\flat[Z_k]} \tag{10}$$

for $u = 1, 2$, and

$$l_2^\flat(z, z'|y) := \begin{cases} \dfrac{Y_2^\flat[Z_k \backslash \{z, z'\}]}{Y_0^\flat[Z_k]} & \text{if} \quad z \neq z', \\ 0 & \text{otherwise.} \end{cases} \tag{11}$$

Assuming that $p_{\text{s},k}(x) = p_{\text{s},k}$ is constant for all $x \in \mathcal{X}$ at time k, the prediction step of the SO-PHD filter is then given by

$$\mu_{k|k-1}(x|y) = \mu_{\text{b},k}(x) + \mu_{\text{s},k|k-1}(x|y), \tag{12}$$

$$\text{var}_{k|k-1}(\mathcal{X}|y) = \text{var}_{\text{b},k}(\mathcal{X}) + \text{var}_{\text{s},k|k-1}(\mathcal{X}|y), \tag{13}$$

where the survival term for the variance $\text{var}_{\text{s},k|k-1}$ is given by

$$\text{var}_{\text{s},k|k-1}(\mathcal{X}|y) = (p_{\text{s},k})^2 \text{var}_{k-1}(\mathcal{X}|y) + p_{\text{s},k}[1 - p_{\text{s},k}]\mu_{k-1}(\mathcal{X}|y). \tag{14}$$

The variance in the number of newborn objects $\text{var}_{\text{b},k}$ is a parameter of the filter, and allows the operator to describe situations where the information on the number of objects entering the image frame.
The Panjer parameters of the predicted object process $\Phi_{k|k-1}$ are then given by [2]

$$\alpha_{k|k-1} = \frac{\mu_{k|k-1}(\mathcal{X}|y)^2}{\text{var}_{k|k-1}(\mathcal{X}|y) - \mu_{k|k-1}(\mathcal{X}|y)}, \tag{15}$$

$$\beta_{k|k-1} = \frac{\mu_{k|k-1}(\mathcal{X}|y)}{\text{var}_{k|k-1}(\mathcal{X}|y) - \mu_{k|k-1}(\mathcal{X}|y)}. \tag{16}$$

With these, the corrective terms $l_u^\flat$ (10), (11) can be computed, and the update step of the SO-PHD follows:

$$\mu_k(x|y) = \mu_{\phi,k}(x|y) l_1^\flat(\phi|y) + \sum_{z \in Z_k} \frac{\mu_{z,k}(x|y)}{s_{\text{ȝ},k}(z|y)} l_1^\flat(z|y). \tag{17}$$

$$\begin{aligned} \text{var}_k(\mathcal{X}|y) = {} & \mu_k(\mathcal{X}|y) + \mu_{\phi,k}(\mathcal{X}|y)^2 \left[l_2^\flat(\phi|y) - l_1^\flat(\phi|y)^2\right] \\ & + 2\mu_{\phi,k}(\mathcal{X}|y) \sum_{z \in Z_k} \frac{\mu_{z,k}(\mathcal{X}|y)}{s_{\text{ȝ},k}(z|y)} \left[l_2^\flat(z|y) - l_1^\flat(\phi) l_1^\flat(z|y)\right] \\ & + \sum_{z, z' \in Z_k} \frac{\mu_{z,k}(\mathcal{X}|y)}{s_{\text{ȝ},k}(z|y)} \frac{\mu_{z',k}(\mathcal{X}|y)}{s_{\text{ȝ},k}(z'|y)} \left[l_2^\flat(z, z'|y) - l_1^\flat(z|y) l_1^\flat(z'|y)\right]. \end{aligned} \tag{18}$$

2.4 Sensor State Estimation

This section focuses on the estimation of the sensor process Ψ. The state of the sensor is denoted by $y \in \mathcal{Y}$, the sensor space $\mathcal{Y}$ describing the relative time difference of an image frame with respect to the previous frame in the image sequence. Following the Sequential Monte Carlo (SMC) implementation in [11], the information regarding the state of the sensor at time k is described by a probability distribution p_k approximated through a set of weighted particles $\{w_k^i, y_k^i\}_{i=1}^N$, i.e.

$$p_k(\cdot) \simeq \sum_{i=1}^{N} w_k^i \delta_{y_k^i}(\cdot). \tag{19}$$

Note that the number of particles, N, is maintained constant throughout the scenario. Selecting an appropriate number of particles is a key consideration of the implementation of the filter. A large number of sensor particles provides a more robust estimator, but increases significantly the computational cost of the overall algorithm: recall from the hierarchical structure (see Sec. 2.2) that a multi-object filter, either a PHD or SO-PHD filter is maintained for each possible sensor state, i.e., for each particle state y_k^i.
By construction, the initial states of y_0^i are uniformly distributed between some lower and upper parameters.
At each time step, the prediction step of the sensor state follows a Markov transition model $h_{k|k-1}$ denoting the operator's knowledge in the nature of the sensor movement (i.e. linear drift). Each particle state is thus resampled according to the transition model, i.e.

$$y_k^i \sim h_{k|k-1}(\cdot|y_{k-1}^i). \tag{20}$$

The update step of the sensor state works as follows. Since the likelihood function $\ell_{z,k}(x|y)$ associating a collected observation z to an object with state x is dependent on the sensor state therefore the estimation of the object process Φ is also conditioned on the sensor state y and is exploited to update the sensor state distribution as follows:

$$w_k^i \propto \frac{\mathcal{L}(Z_k|\Phi, y_k^i) w_{k-1}^i}{\sum_{i=1}^N w_{k-1}^i}, \tag{21}$$

where the *multi-object likelihood* $\mathcal{L}(Z_k|\Phi, y_k^i)$ quantifies the match between the set of collected observations Z_k and the estimation of the object process Φ conditioned on y_k^i. These multi-object likelihoods can be seen below in Sec.2.4.1 and 2.4.2
After the updated weights w_k^i are calculated, the highest weighted particle is found. The resampling step then occurs by uniformly distributing between some minimum and maximum parameters using the highest weighted particle.

2.4.1 PHD Multi-Object Likelihood

If the object process is estimated through a PHD filter (see Sec.2.2.1), the multi-object likelihood is given by [12]:

$$\mathcal{L}(Z_k|\Phi, y_k^i) = \frac{\prod_{z\in Z_k}\left[\mu_{\text{ɜ},k}(z|y_k^i) + \int p_{\text{d},k}(x|y_k^i)\ell_k(z|x, y_k^i)\mu_{k|k-1}(x|y_k^i)\text{d}x\right]}{\exp\left[\int \mu_{\text{ɜ},k}(z|y_k^i)\text{d}z + \int p_{\text{d},k}(x|y_k^i)\mu_{k|k-1}(x|y_k^i)\text{d}x\right]}. \tag{22}$$

2.4.2 SO-PHD Multi-Object Likelihood

If the object process is estimated through a SO-PHD filter (see Sec.2.3), the multi-object likelihood is given by

$$\mathcal{L}(Z_k|\Phi, y_k^i) = \sum_{j=0}^{|Z_k|} \frac{(\alpha_{k|k-1})_j}{(\beta_{k|k-1})^j} \frac{(\alpha_{\text{c},k})_{|Z|-j}}{(\beta_{\text{c},k}+1)^{|Z|-j}} \tilde{F}_{\text{d}}^{-\alpha-j} F_{\text{c}}^{-\alpha_{\text{c},k}-|Z|-j} \sum_{\substack{Z'\subseteq Z_k \\ |Z'|=j}} \prod_{z\in Z'} \mu_{z,k}(\mathcal{X}|y_k^i) \prod_{z'\in Z_k\setminus Z'} \mu_{\text{c},k}(z|y_k^i), \tag{23}$$

where

$$\tilde{F}_{\text{d}} = 1 - \frac{1}{\beta_{k|k-1}} \int p_{\text{d},k}(x|y_k^i) s_{k|k-1}(x|y_k^i)\text{d}x, \tag{24}$$

$$F_{\text{c}} = 1 + \frac{1}{\beta_{\text{c}}}, \tag{25}$$

where $s_{k|k-1}(x|y_k^i) = \dfrac{\mu_{k|k-1}(x|y_k^i)}{\int \mu_{k|k-1}(\bar{x}|y_k^i)\text{d}\bar{x}}$ is the spatial distribution associated to the intensity $\mu_{k|k-1}$.

3 Implementation

All of the multi-object filters used in the experiments are implemented using a Gaussian Mixture (GM) approach following [13], [2] and [9]. Measurement driven birth is also used. Since the parent process is implemented using a SMC particle filter approach, a preset number of particles shall be used.
The motion of the sensor state , herein referred to as the time lapse Δ_k, (20) shall be modelled using two motion models, Brownian motion and static motion, each accounting for a different drift observed in common scenarios. The Brownian motion model, or random walk, describes a scenario where the images are perhaps taken manually by the operator at random intervals. The static model describes a fixed offset with some zero mean Gaussian noise possibly due to a control software error. The time lapse state space is characterised by a simple one dimensional space $x = \Delta_k$. When satellites and debris are observed using telescope, a "streak" is left behind in the image due to the long exposure times needed. The length of this streak can provide an estimate of the target's velocity v, given by:

$$v = \frac{l}{T} \tag{26}$$

Where l and T are the measured streak length and camera exposure time respectively. The inclination (or heading) θ of the streak can also be measured.
This motion using the Nearly Constant Heading (NCH) motion model [14]. It provides a better representation of the target dynamics than a regular Nearly Constant Velocity (NCV) motion model since the targets move along a fairly fixed line. Dynamic targets are described via their x and y position, the speed v and the inclination θ using a four-dimensional state space $\mathcal{X} \subseteq \mathbb{R}^4$, where specific states at time k are of the form

$$x_k = \begin{bmatrix} \mathrm{x}_k, & \mathrm{y}_k, & v_k, & \theta_k \end{bmatrix}^T \tag{27}$$

The motion model for the dynamic objects is non-linear so an Extended Kalman Filter (EKF) [15] is used to propagate through the time steps. It is given as follows:

$$t_k(x_k|x_{k-1}) = \mathcal{N}(x_k; \hat{x}_k, Q_k), \tag{28}$$

where the intermediate state $\hat{x}_k$ is obtained with

$$\hat{x}_k = x_{k-1} + \Delta_k v_{k-1} \begin{bmatrix} \cos(\theta_{k-1}), & \sin(\theta_{k-1}), & 0, & 0 \end{bmatrix}^T, \tag{29}$$

and where Q_k is a covariance matrix of the form:

$$Q_k = \Delta_k \begin{bmatrix} 0 & 0 & 0 & 0 \\ 0 & 0 & 0 & 0 \\ 0 & 0 & \sigma_{v,k}^2 & 0 \\ 0 & 0 & 0 & \sigma_{\theta,k}^2 \end{bmatrix}, \tag{30}$$

where $\sigma_{v,k}$ and $\sigma_{\theta,k}$ are the standard deviations of the velocity and inclination, respectively.

4 Simulations

In order to test the algorithm, several scenarios shall be simulated, each using a different time lapse motion model. This simulated data will be generated as follows. Firstly a number of initial targets are generated N_t, the targets' states are then initialised following the NCH model stated above. The generated $\mathrm{x}_k, \mathrm{y}_k$ positions are limited to within the sensor's FoV, the velocities v_k are drawn from a uniform distribution between some minimum v_k^{min} and maximum v_k^{max} velocity parameters and the inclinations are drawn from a uniform distribution such that $0 \leq \theta_k \leq 360$. As stated before the target transition model follows the NCH model Eq.28. Spontaneous target birth may occur at each time step k and is modelled using a Poisson process with rate λ_b. Target death and detection rates are other factors and they are modelled using Bernoulli processes with probabilities of survival p_s and detection p_d. False alarms may also occur at each time step k, in these simulations a Poisson process with rate λ_{fa} is used to represent these clutter process. The clutter process is also assumed to be uniformly distributed over the entire sensor FoV. At each time step measurements z_k are obtained from the simulated targets' states x_k using the observation model:

$$z_k = H_k x_k + \mathcal{N}(0, R_k), \tag{31}$$

Where H_k is given by

$$H_k = \begin{bmatrix} 1 & 0 & 0 & 0 \\ 0 & 1 & 0 & 0 \\ 0 & 0 & 0 & 1 \end{bmatrix}, \tag{32}$$

And R_k is given by

$$R_k = \begin{bmatrix} \sigma^2_{\mathrm{x},k} & 0 & 0 \\ 0 & \sigma^2_{\mathrm{y},k} & 0 \\ 0 & 0 & \sigma^2_{\theta,k} \end{bmatrix}, \tag{33}$$

For ease of simulation, the exposure time of the camera T is fixed to 1 second. The measured velocity is only used for initialising new targets. The simulation of the time lapse between successive images Δ_k is dependent upon the scenario. It shall be done in one of two ways:

- Static Δ_k : A value of Δ_k is generated at the start of the scenario. This remains constant throughout.
- Random Δ_k : A value of Δ_k is generated at each time step k, drawn from a uniform distribution between some minimum Δ_k^{min} and maximum Δ_k^{max} parameters

The two simulated scenarios share the same parameters with the exception of how the time lapse Δ_k evolves. These parameters are shown below in Table.1

Number of Monte Carlo (MC) Runs	40	Number of MC Particles	50
Number of Time Steps	30	Initial Number of Targets M	10
Rate of Target Birth λ_b	0.2 births / frame	Minimum Target Velocity v_k^{min}	5 pixels/image
Maximum Target Velocity v_k^{max}	15 pixels/image	Survival Probability p_s	0.95
Detection Probability p_d	0.9	False Alarm Rate λ_{fa}	5 / frame
State Space Dimensions ($X \times Y$)	1000 pixels × 1000 pixels	Minimum Time Lapse Δ_k^{min}	0.1 seconds
Maximum Time Lapse Δ_k^{max}	4 seconds		

Table 1 – Simulation parameters

The accuracy of the time lapse estimation shall be measured using the Root Mean Square Error (RMSE) between the estimate obtained from the particle filter and the ground truth. Also the presented results are the averaged results over the MC runs. The estimates used in the results are obtained using a Maximum A Posteriori (MAP) estimate of the posterior likelihood distribution.
The output from the highest weighted particle's PHD or SO-PHD filter, at each time step, shall be compared to the simulated ground truths using the Optimal SubPattern Assignment (OSPA) metric [16]. The OSPA metric introduces the concept of a miss distance for multi-target filters, which jointly weights the accuracy of a filter's spatial estimates and its estimated target cardinality to produce a single value. For the OSPA results shown, a cut-off parameter of $c = 100$m and order parameter $p = 2$ is used. The estimated number of targets alongside the ground truth shall also be shown.

5 Results

The execution times of the methods can be seen in Table.2, as expected the SO-PHD implementation is more computationally expensive by a factor of approximately 1.5. Fig.1 shows the acrmse of the Δk estimates. These show that for both scenarios the Single Cluster Probability Hypothesis Density (SC-PHD) method performs incredibly well (0.086 peak RMSE), regardless of the multi-object filter used. Note that the Δk estimate is highly dependent on the number of particles as more particles will allow a more accurate estiamte to occur.
The OSPA (Fig.2) and estimated cardinality (Fig.3) results show that the estimation of the multi-object state is also accurate, with the filters often being less than 50 for both scenarios. As expected the SO-PHD filter performs better than the PHD filter. Note that the variance estimated by the SO-PHD filter is not shown here.

Method	Random	Static
PHD	0.592	0.612
SO-PHD	0.928	1.095

Table 2 – Execution time results in seconds per time step

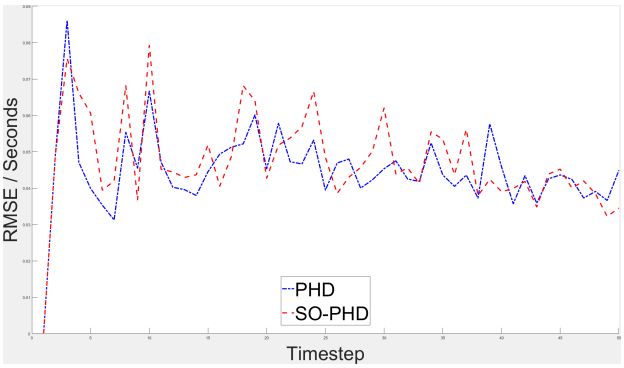

(a) Random Δk Scenario

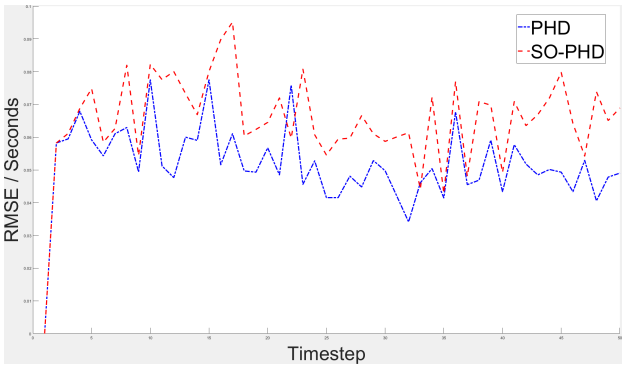

(b) Static Δk Scenario

Figure 1 – RMSE results of the Δk estimates

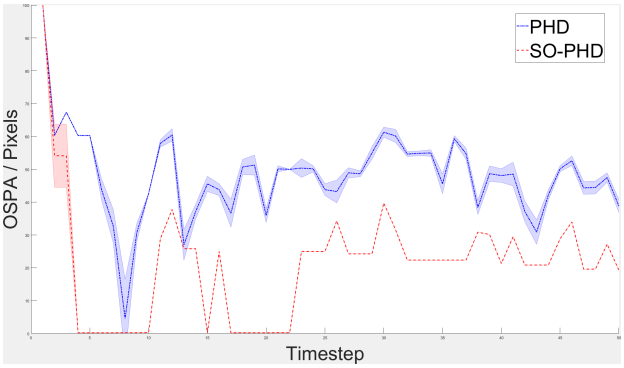

(a) Random Δk Scenario

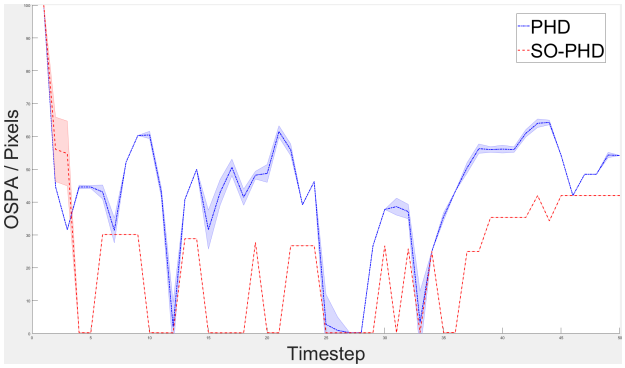

(b) Static Δk Scenario

Figure 2 – OSPA results of the Δk estimates

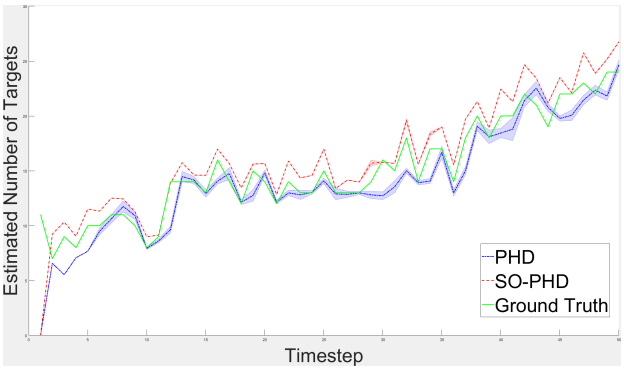

(a) Random Δk Scenario

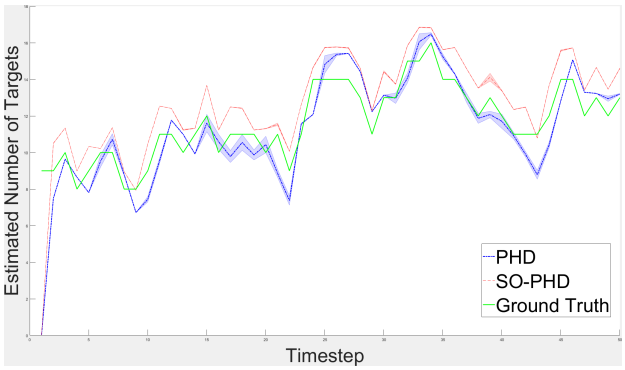

(b) Static Δk Scenario

Figure 3 – Cardinality results of the Δk estimates

6 Conclusions

From the results shown above, it is clear that the Single Cluster Probability Hypothesis Density (SC-PHD) filter can accurately estimate the time lapse that occurs between images whilst also simultaneously tracking the dynamic objects in the image sequence. It has also been shown to work on real data although that is outside the scope of this paper. This method is not just limited to this application, it can be extended to almost any sensor calibration problem.

The main limitation of this implementation is that it requires some measurable information about the targets' velocity or that the targets all move at roughly the same speed. A possible extension to this method can be seen in [4], where a joint update step for the PHD filter is used to discriminate better between the different target populations. the method could be extended to the physical spherical plane (right ascension α and declination δ). This would allow a more meaningful physical interpretation of the results to occur and an easier integration with common orbital determination methods.

7 References

[1] R. P. S. Mahler, "Multitarget Bayes Filtering via First-Order Multitarget Moments," *Aerospace and Electronic Systems, IEEE Transactions on*, vol. 39, no. 4, pp. 1152–1178, 2003.

[2] I. Schlangen, "A Second-Order PHD Filter with Mean and Variance in Target Number," *Accepted to: Transactions on Signal Processing, IEEE Journal of*, 2016. arXiv:1704.02084.

[3] R. P. S. Mahler, "PHD Filters of Higher Order in Target Number," *Aerospace and Electronic Systems, IEEE Transactions on*, vol. 43, no. 4, pp. 1523–1543, 2007.

[4] C. S. Lee, D. E. Clark, and J. Salvi, "SLAM with Dynamic Targets via Single-Cluster PHD Filtering," *IEEE Journal for Selected Topics in Signal Processing (Special Issue on Multi-Target Tracking)*, 2013.

[5] B. Ristic, D. E. Clark, and N. Gordon, "Calibration of Multi-Target Tracking Algorithms Using Non-Cooperative Targets," *Selected Topics in Signal Processing, IEEE Journal of*, vol. 7, no. 3, pp. 390–398, 2013.

[6] I. Schlangen, J. Franco, J. Houssineau, W. T. E. Pitkeathly, D. E. Clark, I. Smal, and C. Rickman, "Marker-Less Stage Drift Correction in Super-Resolution Microscopy Using the Single-Cluster PHD Filter," *Selected Topics in Signal Processing, IEEE Journal of*, vol. 10, pp. 193–202, Feb. 2016.

[7] M. Campbell, I. Schlangen, E. Delande, and D. Clark, "Image Registration Using Single Cluster PHD Methods," in *Advanced Maui Optical and Space Surveillance Technologies Conference*, 2017.

[8] I. Schlangen, *Multi-object filtering with second-order moment statistics.* PhD thesis, Heriot-Watt University, 2017. Ph.D. thesis.

[9] B.-T. Vo, B.-N. Vo, and A. Cantoni, "Analytic Implementations of the Cardinalized Probability Hypothesis Density Filter," *Signal Processing, IEEE Transactions on*, vol. 55, no. 7, pp. 3553–3567, 2007.

[10] I. Schlangen, D. E. Clark, and E. D. Delande, "Single-cluster PHD filter Methods For Joint Multi-Object Filtering and Parameter Estimation," May 2017. arXiv:1705.05312.

[11] C. S. Lee, D. E. Clark, and J. Salvi, "SLAM with Single Cluster PHD Filters," in *Robotics and Automation (ICRA), 2012 IEEE International Conference on*, pp. 2096–2101, May 2012.

[12] A. Swain, *Group and Extended Target Tracking with the Probability Hypothesis Density Filter.* PhD thesis, Heriot-Watt University, 2013.

[13] B.-N. Vo and W.-K. Ma, "The Gaussian Mixture Probability Hypothesis Density Filter," *Signal Processing, IEEE Transactions on*, vol. 54, no. 11, pp. 4091–4104, 2006.

[14] P. A. Kountouriotis and S. Maskell, "Maneuvering Target Tracking Using an Unbiased Nearly Constant Heading Model," in *2012 15th International Conference on Information Fusion*, pp. 2249–2255, July 2012.

[15] B. D. O. Anderson and J. B. Moore, *Optimal Filtering.* Prentice-Hall, 1979.

[16] D. Schuhmacher, B.-N. Vo, and B.-T. Vo, "A Consistent Metric for Performance Evaluation of Multi-object filters," *Signal Processing, IEEE Transactions on*, vol. 56, no. 8, pp. 3447–3457, 2008.